

## 4. RESULTS AND DISCUSSION

### 4.1. Analysis of curcumin

According to USP-32/NF-27; Tumeric *curcuma longa L.* contains not less than 95.0 percent of curcuminoids, as the sum of curcumin, desmethoxycurcumin, and bisdesmethoxycurcumin. It contains not less than 70.0 percent and not more than 80.0 percent of curcumin, not less than 15.0 percent and not more than 25.0 percent of desmethoxycurcumin, and not less than 2.5 percent and not more than 6.5 percent of bisdesmethoxycurcumin.

#### 4.1.1. Analysis of curcumin by HPLC

HPLC chart of curcuminoids was shown in Figure 43. A definite peak was appeared at retention time 18.2 min referred to curcumin. A second peak was appeared at 20.83 min referred to desmethoxycurcumin and a third small peak was appeared at 23.9 min. From HPLC chromatogram, it was concluded the percentage of curcumin peak from the total percentages of curcuminoids was 88.8% while the percentage of desmethoxycurcumin and bisdesmethoxycurcumin peaks were 9.1% and 2.1% respectively. However the amount of each curcuminoids was slightly different from that reported in the USP which might be due to sample purity which was commercially supplied 90-98%.

By examining UV spectrum for each separated peak, it was shown that the three separated peaks have the same UV spectrum indicating the purity of CUR sample and absence of any adulterants as shown in Figure 44.

#### 4.1.2. Identification of curcumin by TLC technique

Thin layer chromatography method was stated in USP 32 for identification of curcuminoids components (i.e. curcumin, desmethoxycurcumin and bisdesmethoxycurcumin) by separation on pre-coated silica gel F<sub>254</sub> plate. Three yellowish brown spots were revealed on TLC plate after elution under UV lamp at wave length 365 nm as shown in Figure 45. By referring to the reference results in USP 32, R<sub>f</sub> values were curcumin > desmethoxycurcumin > bisdesmethoxycurcumin. From these reference results it was concluded appearance of curcumin (spot A) at the top followed by desmethoxycurcumin (spot B) then bisdesmethoxycurcumin (spot C).

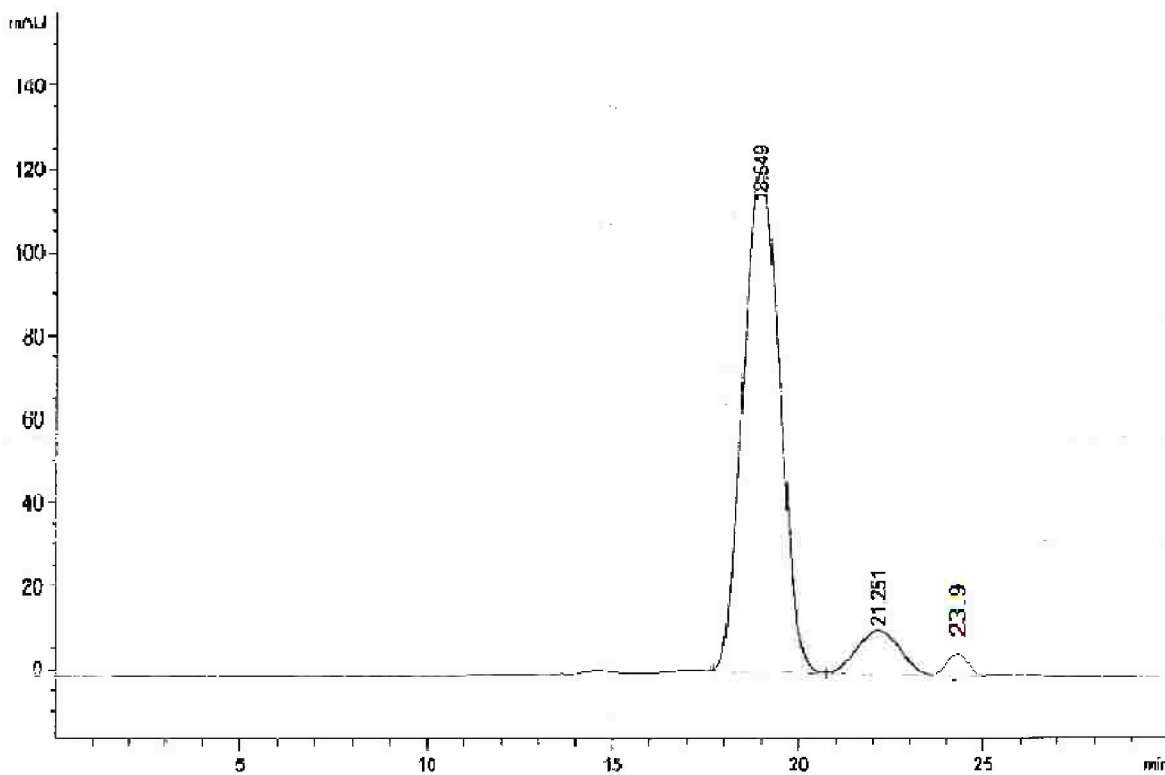


**Figure 43: HPLC chromatogram of curcumin, desmethoxycurcumin and bisdesmethoxycurcumin.**

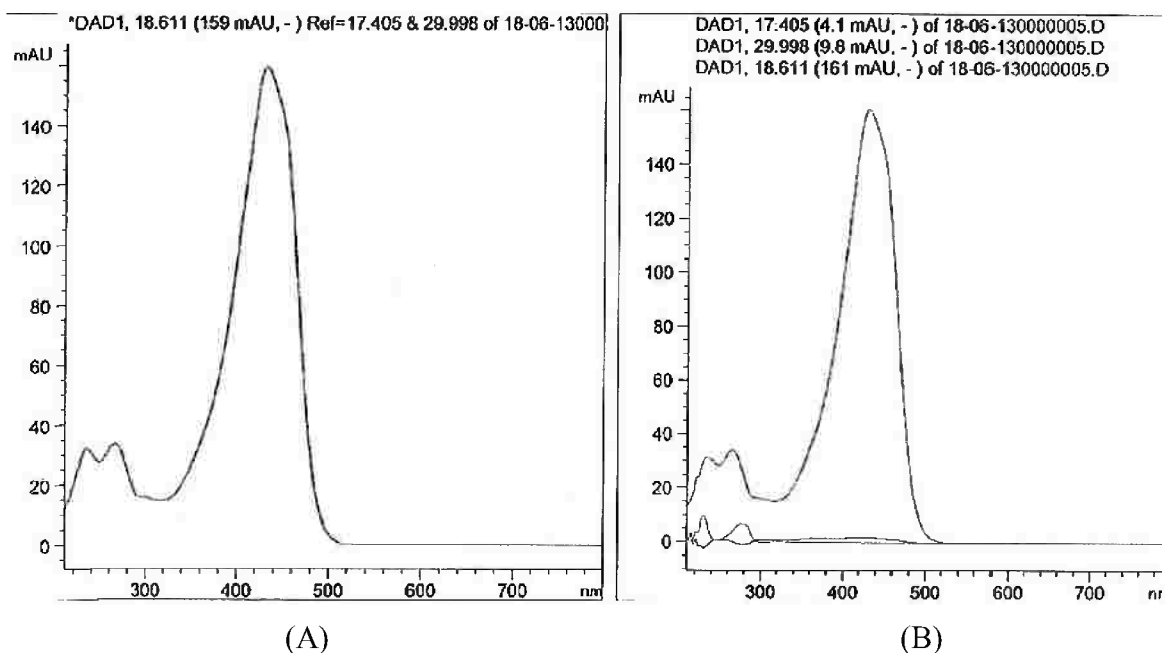


**Figure 44: UV spectra of curcumin (A) and desmethoxycurcumin (B) at wave length 420 nm**

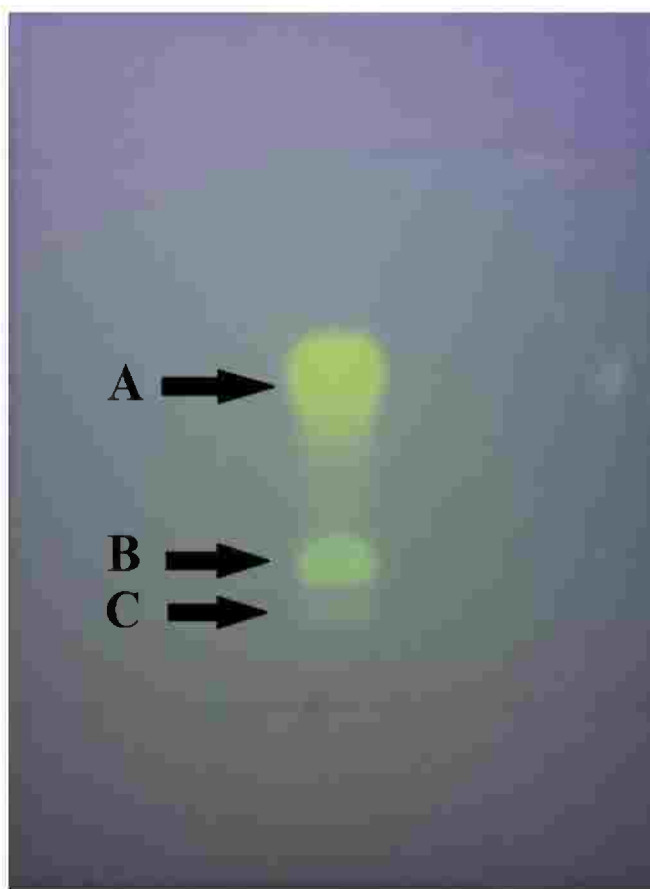


**Figure 45: TLC plate showing (A) curcumin spot, (B) desmethoxycurcumin spot and (C) bisdesmethoxycurcumin under UV-lamp at wave length 365 nm.**

## 4.2. Solubility study of curcumin

Solubility studies were carried out for CUR in different aqueous and non aqueous media. Saturated solubility of CUR in water couldn't be detected spectrophotometrically because of spectrum shift from wave length 420 nm to 280 nm due to its poor stability and decomposition in neutral-basic conditions<sup>(121, 190)</sup>. On the other hand, CUR exhibited better solubility results in aqueous media with application of anionic (i.e. SLS) at different concentrations and non-ionic surfactant (i.e. Tween 80) as shown in Table 3. The results were 0.09, 0.14, 0.35, 0.15 mg/gm CUR for 0.25%, 0.5%, 1% SLS and 0.5% Tween 80 respectively. It was reported that CUR solubility and stability greatly enhanced in the presence of surfactant micellar solutions formed above its CMC<sup>(191)</sup> due to encapsulation of CUR inside the formed micelle<sup>(192, 193)</sup>.

For non-aqueous media results revealed that saturated solubility of CUR in medium chain triglyceride (i.e. Miglyol 812) was higher than saturated solubility in long chain triglycerides (i.e. soya bean oil) to be 1.56 and 0.14 mg/gm respectively.

Solubility results for CUR in hydrophilic surfactants as CRM EL and KLS P 124 were found to reach 41 and 1.23 mg/gm respectively as shown in Table 14.

### 4.3. Preparation of CUR-SPC S 100 complex (CUR phytosome)

Maiti *et al*<sup>(129)</sup> and Gupta *et al*<sup>(158)</sup> mentioned a method for preparation of CUR-SPC complex by a solvent evaporation method. The preparation procedure was summarized in 3 steps. Step1 is refluxing of CUR and SPC in a common organic solvent able to solubilize both ingredients for a definite time. Step2 is a removal of the organic solvent by a rotary evaporator. Step 3 is washing out the excess of SPC with n-hexane resulting in the formation of CUR-SPC complex in a semisolid form. Industrially, the previous mentioned method couldn't be applied to produce a commercial form for CUR-SPC complex to be used as a dosage form (i.e. Hard gelatin capsule or soft gelatin capsule). For this purpose, Indena SpA patently produced a commercial powder for CUR-SPC complex with application of 2 parts of microcrystalline cellulose to be filled in a hard gelatin capsule. To produce a locally made CUR-SPC complex powder similar to that prepared by Indena SpA, Step 1 and 2 were applied as directed and a very low density powder (i.e. Aerosil 200) was selected among different fillers to be the most proper filler used as a carrier for CUR-SPC complex instead of microcrystalline cellulose to produce a CUR-SPC complex powder. By application of a controlled temperature water bath adjusted at 45-50°C, dichloromethane was evaporated completely from the formed flakes after 4-5 hours knowing that the boiling point of the used organic solvent is 39°C. On the other hand, the applied temperature should be controlled as SPC may decompose at high temperature<sup>(194)</sup>. Mechanical grinding by mortar and pestle was applied on the formed complex flakes to produce fine and flowable particle as shown in (Figure 46).

**Table 14: Solubility results of CUR in different vehicles and surfactants**

<b>Material</b>	<b>Solubility of CUR (mg/gm)</b>
<b>0.25% SLS/Water</b>	0.09
<b>0.5% SLS/Water</b>	0.14
<b>1% SLS/Water</b>	0.35
<b>0.5% Tween 80/Water</b>	0.15
<b>Soya bean oil</b>	0.4
<b>Miglyol 812 oil</b>	1.56
<b>Oleic acid</b>	0.4
<b>PEG 400</b>	114.6 <sup>(157)</sup>
<b>Castor oil</b>	0.267 <sup>(156)</sup>
<b>CRM EL</b>	41
<b>KLS P 124</b>	18

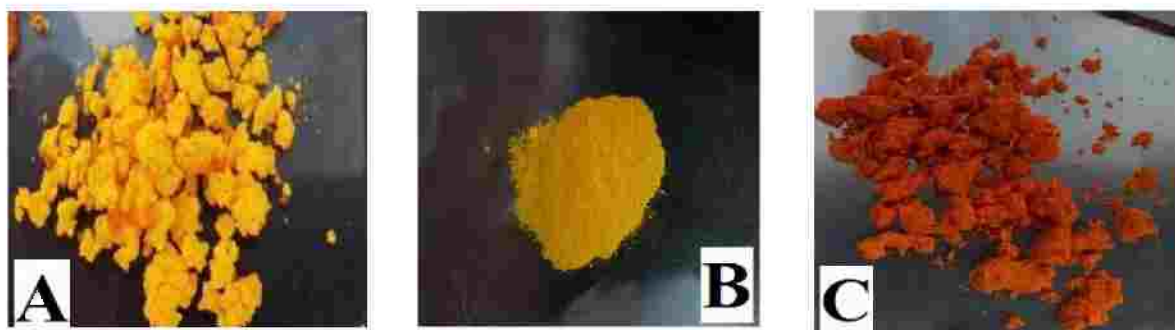


**Figure 46: Prepared CUR-SPC complex powder before grinding (A), after grinding (B) and Meriva™ (C).**

#### **4.4. Characterization of prepared CUR-SPC complex in comparison to Meriva™**

##### **4.4.1. Analysis of CUR content in the prepared complex powder**

Analysis was carried out for the total curcuminoids in the test samples. Results revealed that total curcuminoids in Meriva™ was 19.3% while the prepared complex powder was 19.06%. The content of total curcuminoids in CUR-SPC complex powder depend on the amount of filler used in the preparation; for Meriva™ 2 parts of microcrystalline cellulose used in the preparation to make the ratio among CUR, SPC and microcrystalline cellulose (1:2:2). On the other hand, locally made CUR-SPC complex powder was prepared to deliver the same amount of curcuminoids used in Meriva™ by using Aerosil 200 as a carrier with the same ratio. The amount of curcuminoids in CUR-SPC complex powder may be increased by decreasing the amount of the used filler which requires further examinations.

##### **4.4.2. Differential scanning Calorimetry (DSC)**

DSC is a fast and a crucial tool to screen drug-excipient compatibility and possible interactions at solid state of matter. An interaction is concluded by elimination of endothermic peak(s), appearance of new peak(s), change in peak shape and its onset, peak temperature/melting point and relative peak area or enthalpy. Consequently, DSC thermograms of CUR (A), SPC (B), locally prepared complex (C) and Meriva™ (D) were demonstrated at (Figure 47). The thermogram of pure CUR showed a melting range from 177.6 - 185.3°C with one single peak. Thermogram of SPC showed two different melting ranges; the first one is mild from 154.3 - 160°C and the second one is broad from 232.6 - 295.7°C, which may be due to the movement of phospholipids polar head group and phase transition from gel to liquid crystalline state, respectively as reported in many literatures<sup>(129, 158, 171, 195)</sup>. A melting range from 134.7- 171°C was appeared in the thermogram of locally prepared complex, which was different from each individual components of the complex. This could be due to complete and strong complex formation of CUR with SPC during the preparation process. The -OH groups of the phenol rings of CUR are involved in hydrogen bonding whereas the aromatic rings could be involved in hydrophobic interaction<sup>(129)</sup>. For Meriva™, a similar melting range to that of locally prepared phytosomes was observed from 137.7 - 164°C with small minor peaks which could be attributed to uncomplexed SPC or incomplete evaporation of residual solvent during the preparation process.

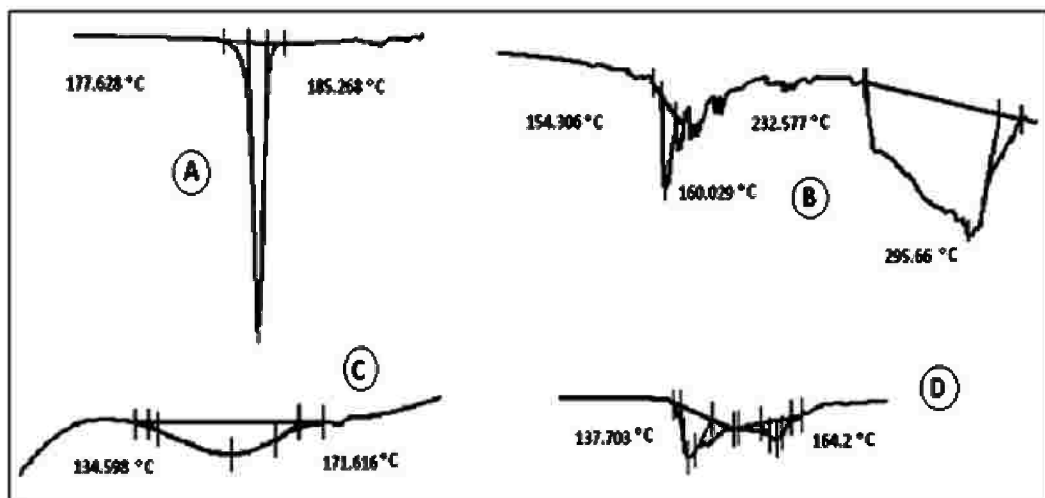


**Figure 47: DSC thermograms exhibiting the peak transition of pure CUR (A), SPC (B), locally prepared complex (C) and Meriva™ (D).**

#### 4.4.3. Fourier Transform Infrared Spectroscopy (FT-IR)

##### 4.4.3.1. (FT-IR) measurement for prepared complex and Meriva™

Further investigations for complex formation were carried out by using infrared spectra spectroscopy. As shown in (Figure 48), the band at  $3501\text{ cm}^{-1}$  was attributed to the stretching vibration of the phenolic  $-\text{OH}$  group in natural CUR (A), additionally two bands were observed at  $1625\text{ cm}^{-1}$  and  $1275\text{ cm}^{-1}$  which attributed for  $\text{C}=\text{O}$  and  $\text{C}-\text{O}$  respectively<sup>(196)</sup>. For SPC (B)<sup>(132)</sup>, strong peaks at  $1736\text{ cm}^{-1}$  and  $1238\text{ cm}^{-1}$  were due to  $\text{C}=\text{O}$  absorption and  $\text{P}=\text{O}$  absorption respectively, strong peaks at  $2925\text{ cm}^{-1}$  and  $2855\text{ cm}^{-1}$  and weak peak at  $1376\text{ cm}^{-1}$  could be due to stretching and deformation of methyl groups. The peak at  $1465\text{ cm}^{-1}$  observed in SPC could be due to bending vibration of  $\text{CH}_2$ <sup>(132)</sup>.

A shift from  $3500\text{ cm}^{-1}$  to broad peak at  $3345\text{ cm}^{-1}$  and  $3403\text{ cm}^{-1}$  for Meriva™ (C), prepared complex (D) respectively which indicates an interaction was taken place at the phenolic  $-\text{OH}$  group while a shift from  $1236\text{ cm}^{-1}$  to  $1267\text{ cm}^{-1}$  for Meriva™ (C) for SPC indicates an interaction between  $\text{P}=\text{O}$  group of SPC and phenolic  $-\text{OH}$  of natural curcumin. For prepared complex (D), a strong broad sharp peak was observed at  $1096\text{ cm}^{-1}$  which may attribute to  $\text{SiO}_2$  group of colloidal silicon dioxide used in the preparation of CUR-SPC complex. This observed peak may mask a peak of  $\text{P}=\text{O}$  of SPC at  $1267\text{ cm}^{-1}$ .

##### 4.4.3.2. (FT-IR) measurement of prepared complex with 1% SLS and 0.5% Tween 80

Interaction of surfactants with simplified membrane models such as phospholipids<sup>(197-199)</sup> leading to breakdown the lamellar structure and formation of lipid- surfactant mixed micelle systems was reported in many literatures<sup>(200)</sup>. Effect of nonionic/anionic surfactants on CUR-SPC complex was examined by application of FT-IR measurements.

(Figure 49) showed that there was no effect of anionic surfactant as SLS (B) or nonionic surfactant as Tween 80 (C) on CUR-SPC complex integrity. Thus, using either of them as a component of dissolution media in the following studies doesn't affect on the CUR-SPC complex.

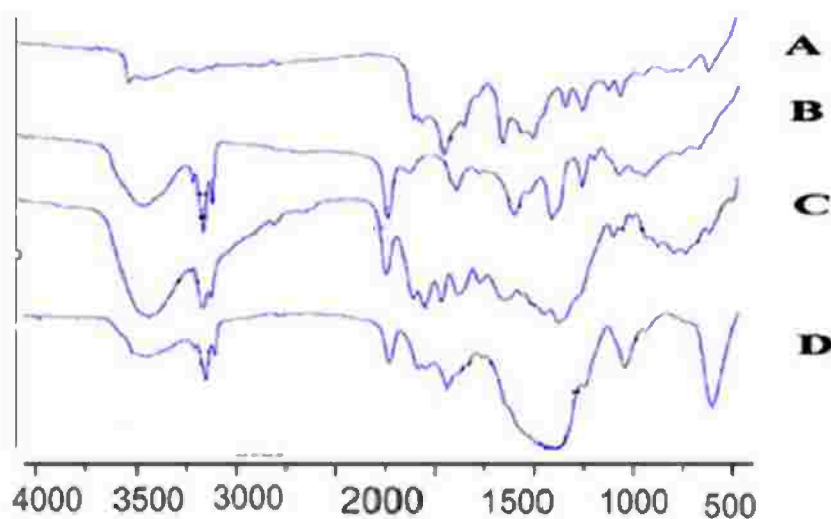


**Figure 48: FTIR spectra of (A) curcumin, (B) phospholipids, (C) Meriva™ and (D) prepared CUR-SPC complex.**

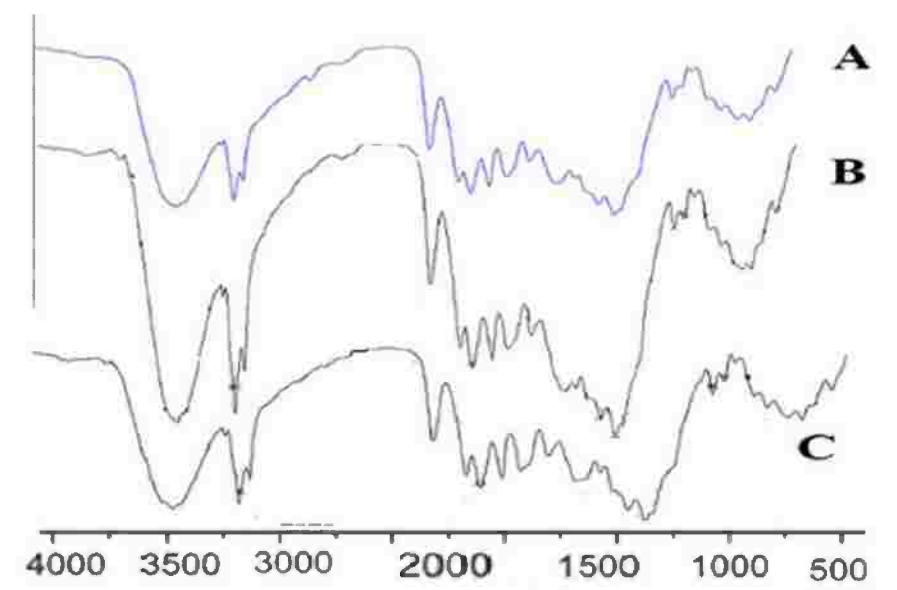


**Figure 49: FT-IR spectra of (A) prepared phytosome, (B) prepared phytosome treated with aqueous 1% SLS and (C) prepared phytosome treated with aqueous 0.5% Tween 80.**

#### **4.4.4. Measurement of zeta- potential (ZP)**

The magnitude of zeta potential indicates the degree of electrostatic repulsion between similarly charged particles which affects the stability of colloidal dispersions. Phytosomes carry a negative charge due to the presence of SPC phosphate groups in a water environment at a neutral pH value<sup>(201)</sup>. Results revealed that ZP measurement between Meriva™ (A) and locally prepared complex (B) was -33.8 mV, -35.4 mV respectively as shown in (Figure 50).

#### 4.4.5. Transmission electron microscopy (TEM) and particle size determination.

Mean particle size (PS) could not be determined by using dynamic light scattering technique due to the presence of water insoluble fillers like microcrystalline cellulose in Meriva™ and colloidal silicon dioxide in the locally prepared complex suspended in the test sample leading to positive error in the readings. From this point of view, PS was determined by using TEM. (Figure 51) revealed a formation of small round vesicles of CUR phytosome from Meriva™ with mean PS  $37.2 \pm 7.07$  nm on dispersion in distilled water. While in (Figure 52), it was shown a small round vesicles formation of CUR phytosome from the locally prepared complex with mean PS  $24.2 \pm 1.66$  nm.

#### 4.4.6. Scanning electron microscopy (SEM)

(Figure 53(a)) showed irregular cylindrical shaped and rough crystalline form of CUR powder which lines with observation by paradkar *et al* (202). On other hand, (Figure 53 (b, c)) showed an irregular, round shaped and smooth surface CUR-SPC complex for Meriva™ and locally prepared product which could be attributed to change in internal crystalline structure due to complex formation.

#### 4.4.7. Thin layer chromatography technique (TLC)

It was shown that the evaluation of complex formation on comparing Meriva™ and locally prepared phytosome will depend on the difference in the place of pure SPC spot (A) in comparing with Meriva™ spot place (B) samples and prepared complex spot place (C). By examination of TLC plate as shown in (Figure 54), it was observed similarity of SPC spot place between Meriva™ (B) and prepared complex (C) which in turns confirm the complex formation and similarity between the two latter samples.

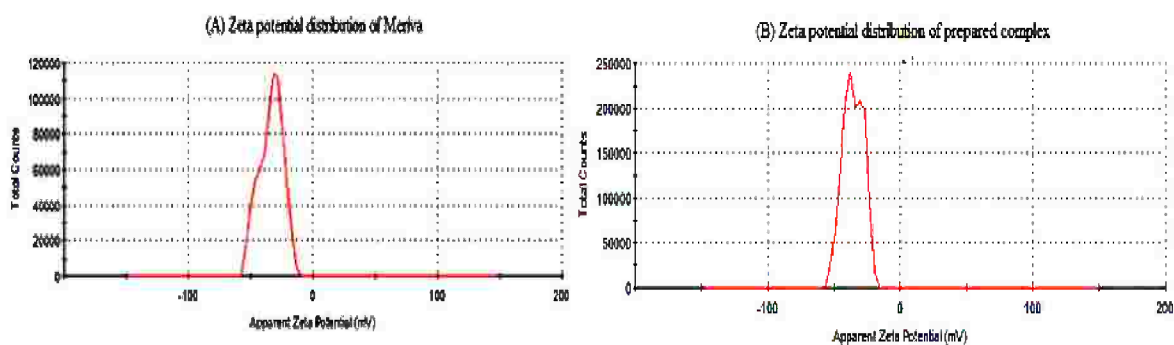


**Figure 50: ZP measurements of Meriva™ (A) and prepared CUR-SPC complex (B)**

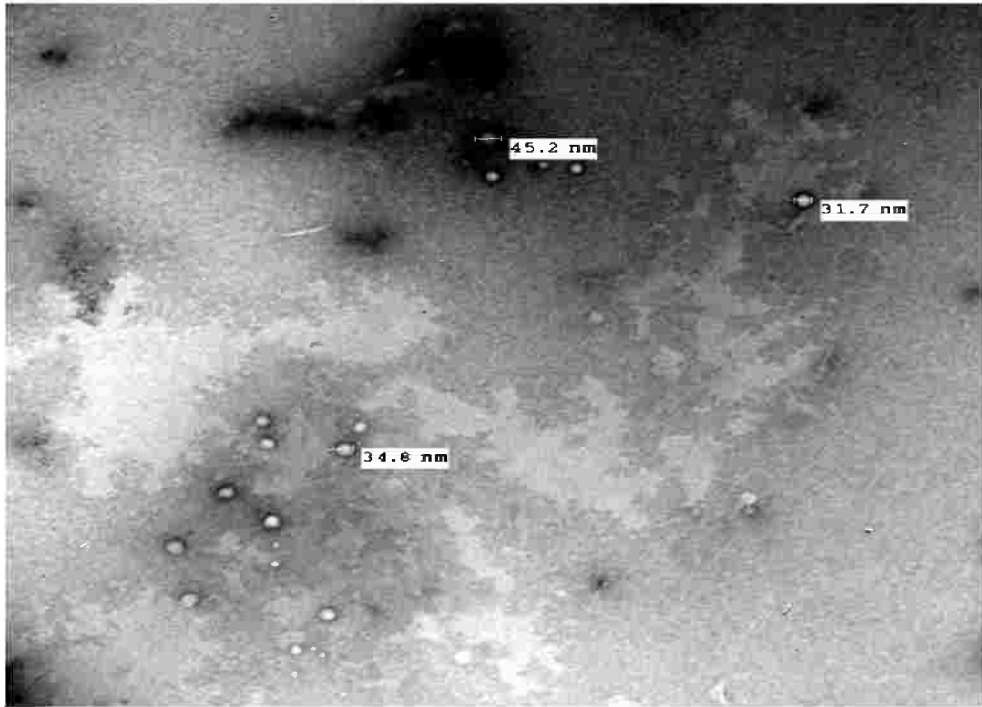


**Figure 51: Transmission electron microscopic photograph of Meriva™ with 20 folds dilution in distilled water**

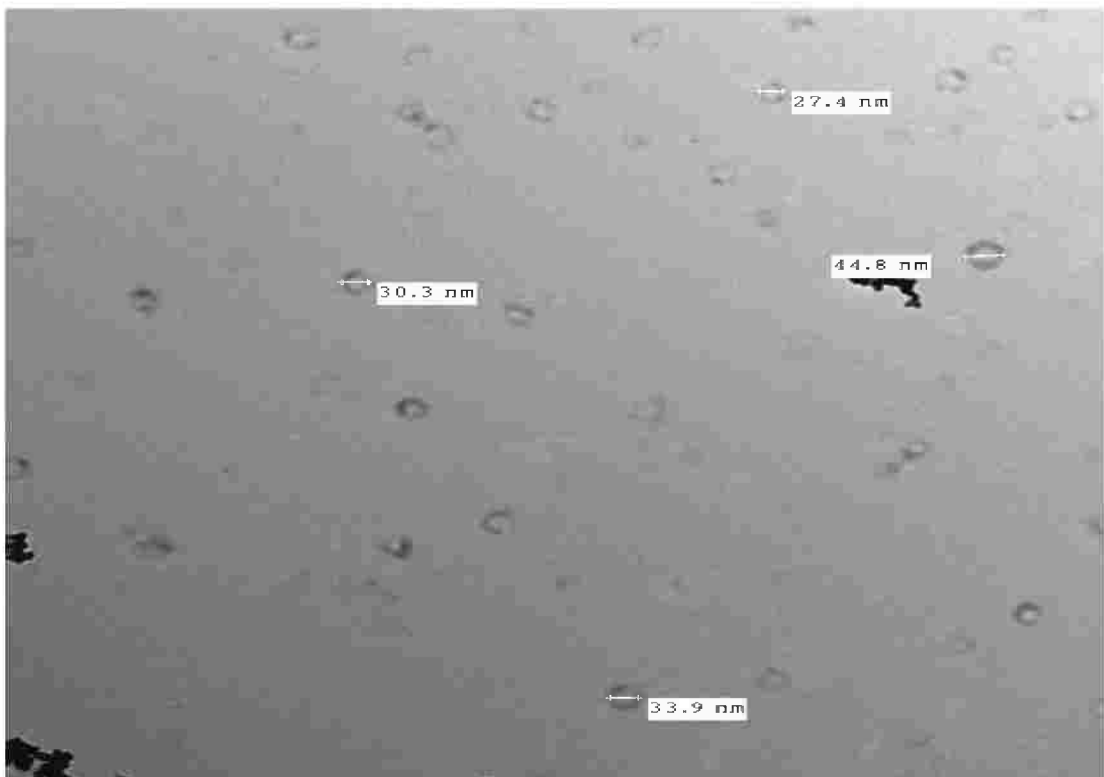


**Figure 52: Transmission electron microscopic photograph of locally prepared phytosome with 20 folds dilution in distilled water.**

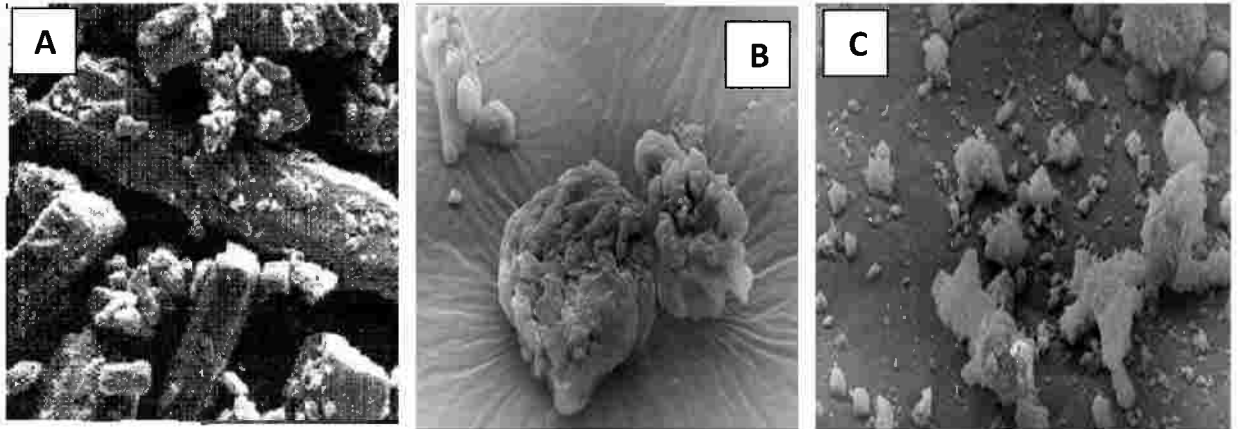


Figure 53: Scanning electron microscope photograph of (A) CUR, (B) Meriva™ and (C) locally.

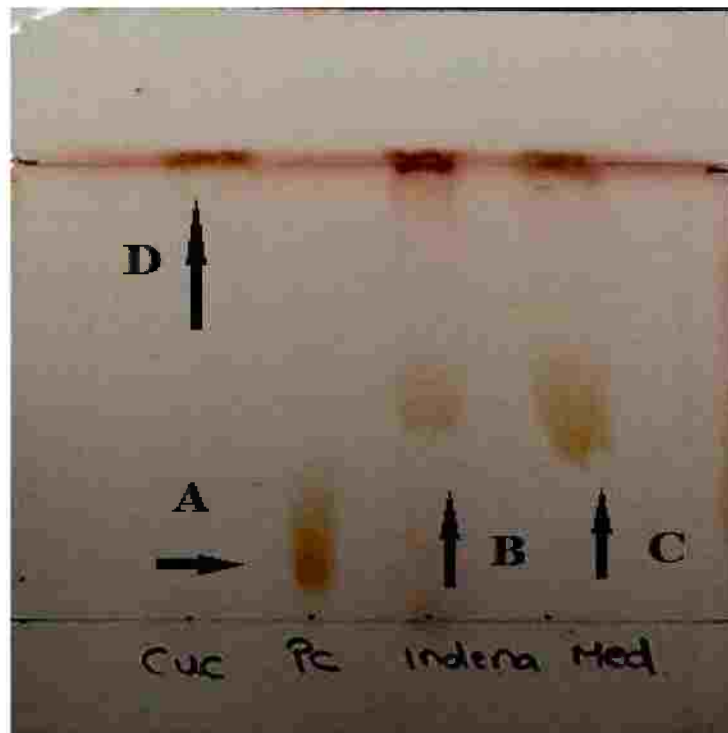


Figure 54: TLC plate showing (A) pure SPC spot, (B) SPC spot for Meriva™, (C) SPC spot for prepared complex and (D) spot for pure CUR.

#### 4.4.8. *In vitro* dissolution study

Despite of the reported effect of SLS on phospholipids in presence of water <sup>(200)</sup>, USP 32 recommended the use of 1% SLS as a dissolution medium for CUR powder. Our FT-IR results showed that there was no effect of either anionic or nonionic surfactant on CUR-SPC complex integrity. This was because of the absence of a specified dissolution medium for CUR-SPC complex, different dissolution media (0.25%, 0.5% & 1%) SLS and 0.5% Tween 80<sup>(129)</sup> were used to study the dissolution pattern for CUR-SPC complex for 4 hours at the same pharmacopeial conditions. By using the above mentioned dissolution systems, a comparative in-vitro dissolution study were carried out between Meriva<sup>TM</sup> and the locally prepared complex.

As shown in (Figure 55), dissolution profile for CUR powder couldn't be measured in 0.25% SLS medium due to limited solubility of CUR in 0.25% SLS if compared to other dissolution media. As a general pattern, on increasing the SLS concentration, the dissolution profile for CUR in its complexed powder form was enhanced due to better wettability for the complex powder resulting in better dissolution profile (Figures 55-57).

Locally prepared complex powder demonstrates better dissolution profile than Meriva<sup>TM</sup> as shown in (Figures 55, 56 and 57) for 0.25%, 0.5% and 1% SLS respectively, this may be due to better wettability of free flowing prepared complex powder with experimental determined particle size (i.e. less than 75  $\mu\text{m}$ ) than Meriva<sup>®</sup> powder with particle size (i.e. more than 75 $\mu\text{m}$ ) indicating the unsuitability of 1% SLS dissolution system to compare prepared complex powder with Meriva<sup>TM</sup>. On other hand, dissolution profile of prepared complex powder is very similar to Meriva<sup>TM</sup> in 0.5% Tween 80 (Figure 58).

Dissolution profiles shown at (Figures 56 and 58) indicate a similar dissolution profile for both CUR-SPC complex powder on using 0.5% SLS and 0.5% Tween 80. These indicate that the change in the type of surfactant doesn't affect the dissolution profile but a change in the surfactant concentration has an effect on the dissolution profile for CUR-SPC complex powder.

It should be mentioned that the dissolution profile for CUR-SPC complex powder in all dissolution media is failed to achieve the pharmacopeial tolerance which is stated to be not less than 75% after 1 hour at all surfactant concentrations indicating a need for a further formulation development for CUR-SPC complex powder to achieve the pharmacopeial limit.

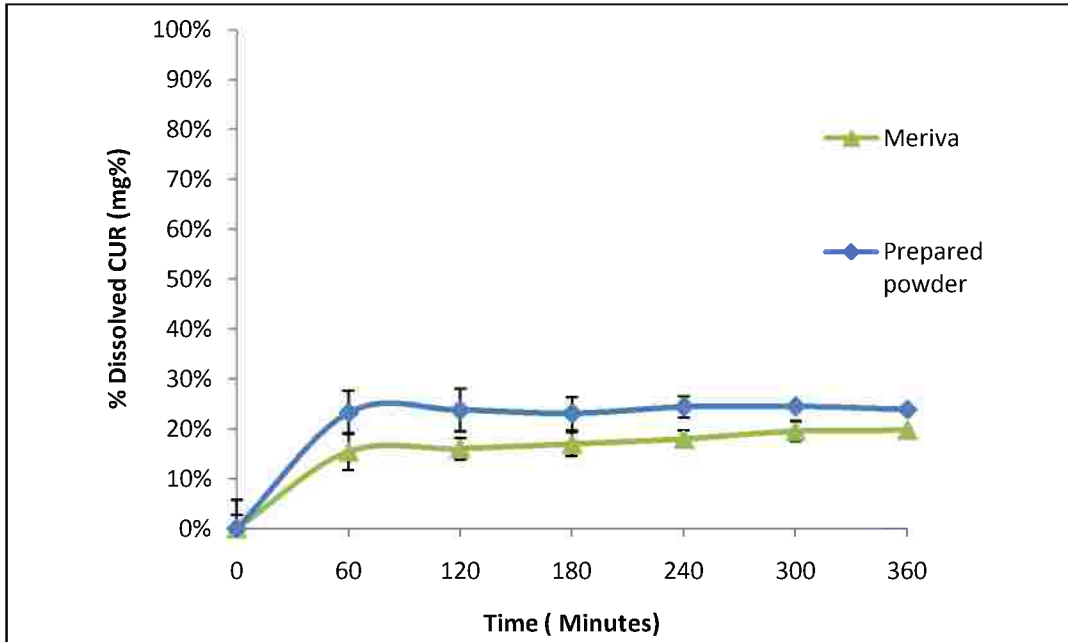


**Figure 55: Comparative dissolution profile between Meriva™ and prepared complex powder 0.25% aqueous SLS.**

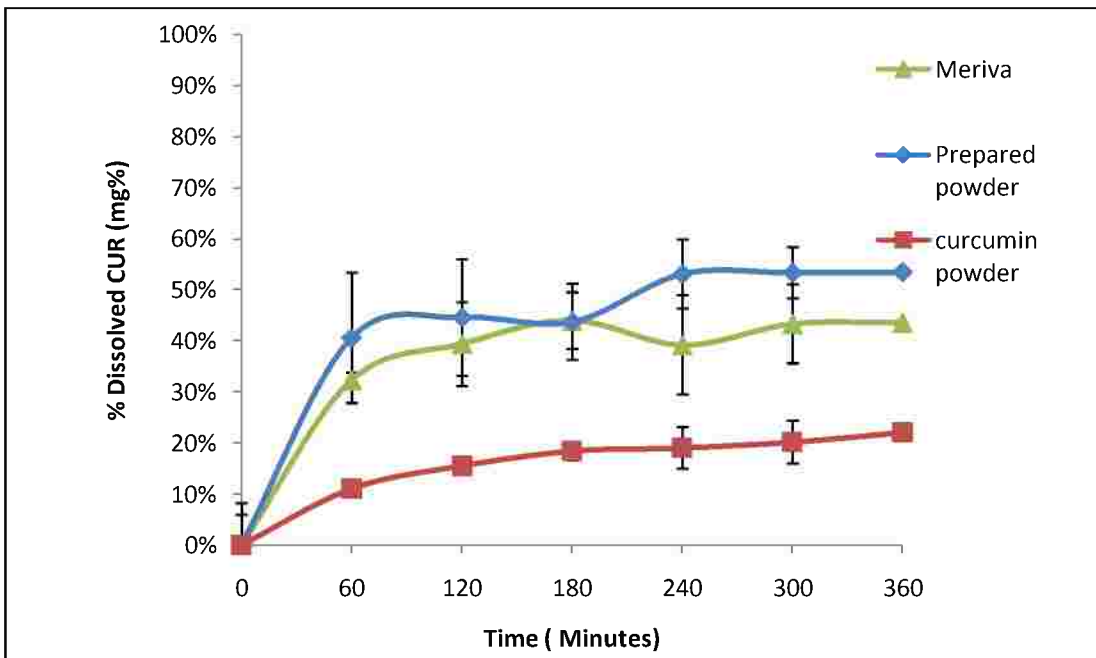


**Figure 56: Comparative dissolution profile between Meriva™, prepared complex powder and pure CUR powder in 0.5% aqueous SLS.**

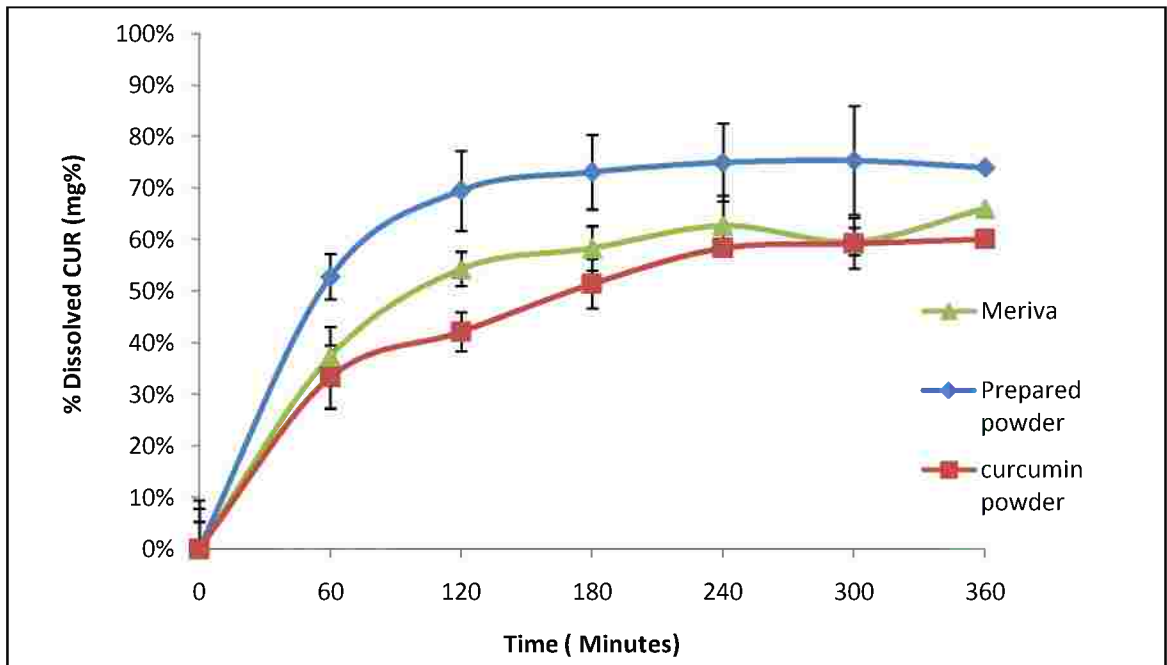


**Figure 57: Comparative dissolution profile among Meriva™, prepared complex powder and CUR pure powder in 1% aqueous SLS.**

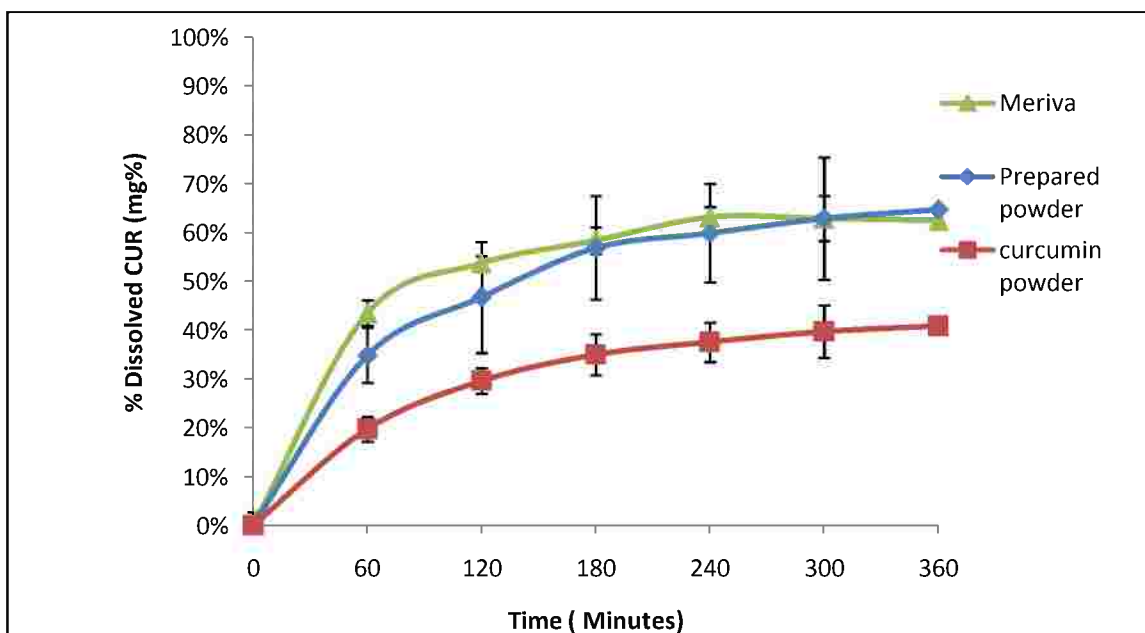


**Figure 58: Comparative dissolution profile among Meriva™, prepared complex and CUR pure powder in aqueous 0.5% Tween 80.**

#### 4.4.9. *Ex vivo* intestinal permeation studies

*In vitro* absorption models as non-everted intestinal sac was commonly used to study drug absorption<sup>(203)</sup> through the intestine which reflects the in-vivo drug absorption in humans with less labor and experimental costs to be compared with in vivo studies. For passive transported drugs (i.e. No energy required for permeation), Genty *et al*<sup>(204)</sup> reported the permeability of passive absorption drug remained the same whether the sacs were everted or not. These results support the use of non-everted sac model to study the permeation of passively diffused CUR<sup>(137)</sup>. Several advantages to utilize non everted sac model over everted sac model including simplicity, need for less amount of test sample and ability to collect successive of serosal samples with less morphological changes<sup>(205)</sup>.

##### 4.4.9.1. Preparation of receiver solution and test samples

Although Gupta *et al*<sup>(158)</sup> utilized everted intestinal sac model to study the permeation difference between CUR-SPC complex and CUR powder, the design of the used system must be criticized. This is due to two reasons:

1. Addition of CUR powder in phosphate buffered saline with pH 7.4, knowing the reported instability of CUR powder in alkaline medium<sup>(121)</sup>.
2. Long period of the experiment time up to 6 hours with an absence for any data guarantee the intestine viability for a long period of time.

On other hand Shishu *et al*<sup>(206)</sup> also utilized non-everted intestinal sac model to show effect of different vehicles on the permeation of CUR from various sources where the receiving solution compromised from Ringer phosphate buffered saline at pH 7.4 and isopropyl alcohol in ratio (7:3), but the design of the experiment must be criticized due to three reasons:

1. Utilizing a receiving solution contain an alkaline phosphate buffered saline with pH 7.4 will lead to a chemical decomposition of the permeated CUR which promotes a false negative results especially the analysis was taken place by spectrophotometer.
2. Absence of an evidence data that using a strong dehydrating agent as isopropyl alcohol will affect on intestine viability which may lead to false results.
3. Long period of time to perform the experiment reaching to 8 hours with an absence for any data guarantee the intestine viability to stand for such period of time.

Because of the above mentioned criticism, it was concluded that there were a need to create a new experiment design depending on data published by Hamid *et al*<sup>(207)</sup> about the effect of different solubilizing agents on the intestine viability of rat. Various solubilizing agents were tested according to their ability to solubilize CUR including 10% PEG 400, 10% Ethanol and 10% Cremophore EL. From this point of view, 10% CRM EL showed the highest solubilizing effect for CUR to be mixed with saline solution containing 2% Ethanol to form the receiver solution for ex-vivo permeation study.

##### 4.4.9.2. Preparation of test samples

According biopharmaceutical classification system (BCS), CUR was classified by Wahlang *et al*<sup>(137)</sup> as class IV, possess poor solubility and poor permeability. Poor permeability of CUR was encountered due to intestinal metabolism by CYP 3A4 enzymes resulting in formation of curcumin glucouronide and curcumin sulphate metabolites<sup>(131)</sup>. To avoid any obstacle may

interfere with CUR permeability through non everted rat intestine, 100  $\mu\text{m}$  itraconazole which is reported to be CYP 3A4 inhibitor<sup>(137)</sup> was added to dispersion solution for test samples before the injection process. On other hand, 2% Tween 80 (i.e. has no effect on intestinal viability of rats)<sup>(207)</sup> was added as a wetting agent for Meriva<sup>TM</sup> and locally prepared complex powder to enhance the dispersion of the powder in the prepared solution.

#### 4.4.9.3. Experimental results

##### 4.4.9.3.1. Permeation results

Results revealed a similarity between the amounts of CUR permeated across rat intestine in terms of micro grams ( $\mu\text{g}$ ) from Meriva<sup>TM</sup> and the locally prepared CUR-SPC complex as shown in (Figure 59), where it was shown that the maximum permeability of CUR was reached to 45  $\mu\text{g}$  after 60 mins in the receiver compartment and there was no increase of the permeability until 180 min. These results may be due to CUR entrapment being lipophilic in nature inside the intestinal mucosal cells leading to limited CUR permeation across rat intestine. On the other hand, permeability results of CUR suspension across rat intestine was 11  $\mu\text{g}$  after 3 hours. It is concluded that complexation of CUR with phospholipid leading to enhance permeation of CUR 4 times if compared with corresponding CUR suspension.

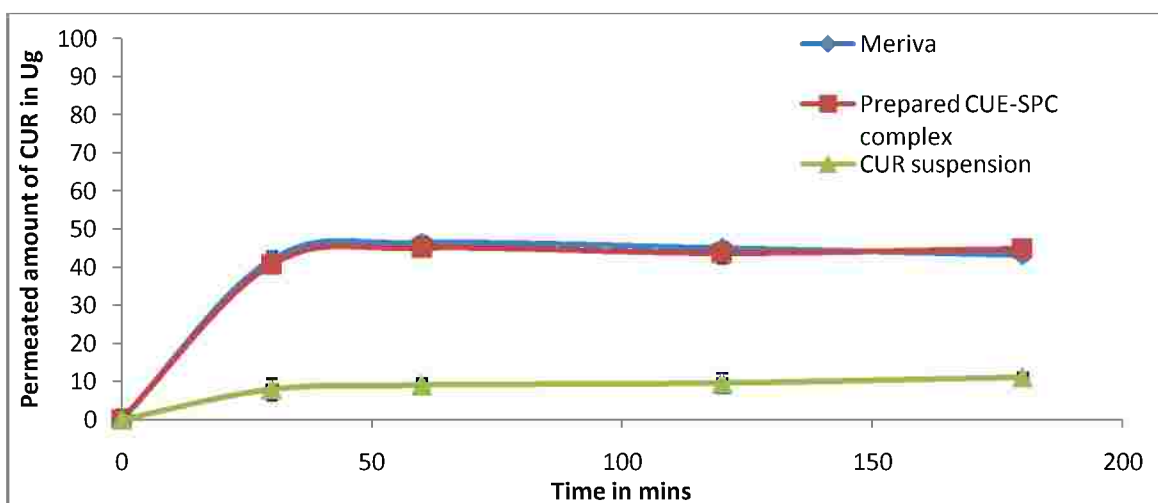


**Figure 59: Comparative permeation results of Meriva<sup>TM</sup>, prepared CUR-SPC complex and CUR suspension.**

A similar work was reported by Freag *et al*<sup>(185)</sup> to study the permeability difference between diosmin phytosomes and diosmin powder suspension utilizing non everted sac model, % diosmin permeated showed a short lag period within 40 mins then increased to reach more than 80% after 2 hours while for CUR phytosome, a relative much lower results was obtained. This may be related to a drug-phospholipid complex integrity where previous experiments proved a strong complex formation between CUR and phospholipid in contrary to diosmin-phospholipid complex which showed a weak complex form. From this point of view, it is suggested that a strong complex integrity between CUR and phospholipid and high lipophilicity of CUR phytosome leading to retention of CUR-SPC complex in mucosal cells hence provides much lower permeation results on comparing with diosmin phytosome.

#### 4.4.9.3.2. Mucosal uptake results

Results obtained from the analysis of the amount of CUR retained inside the mucosal cells (i.e. mucosal uptake) illustrated in (Figure 60) revealed a similarity between Meriva™ and the prepared complex powder in mucosal uptake of the rat intestine.

In the contrary, mucosal uptake for CUR suspension was much higher than those obtained from application of CUR in its phytosomal structure. This may be encountered to a high lipophilicity and low aqueous solubility of CUR powder leading to attachment of CUR to the outside part of the mucosal cells resulting in low permeation of CUR across the rat intestine. Phytosomal structure of curcumin either for Meriva™ or prepared CUR SPC complex increase intestinal permeation of curcumin compared to CUR suspension which subsequently decrease CUR appendance inside the mucosal cells.

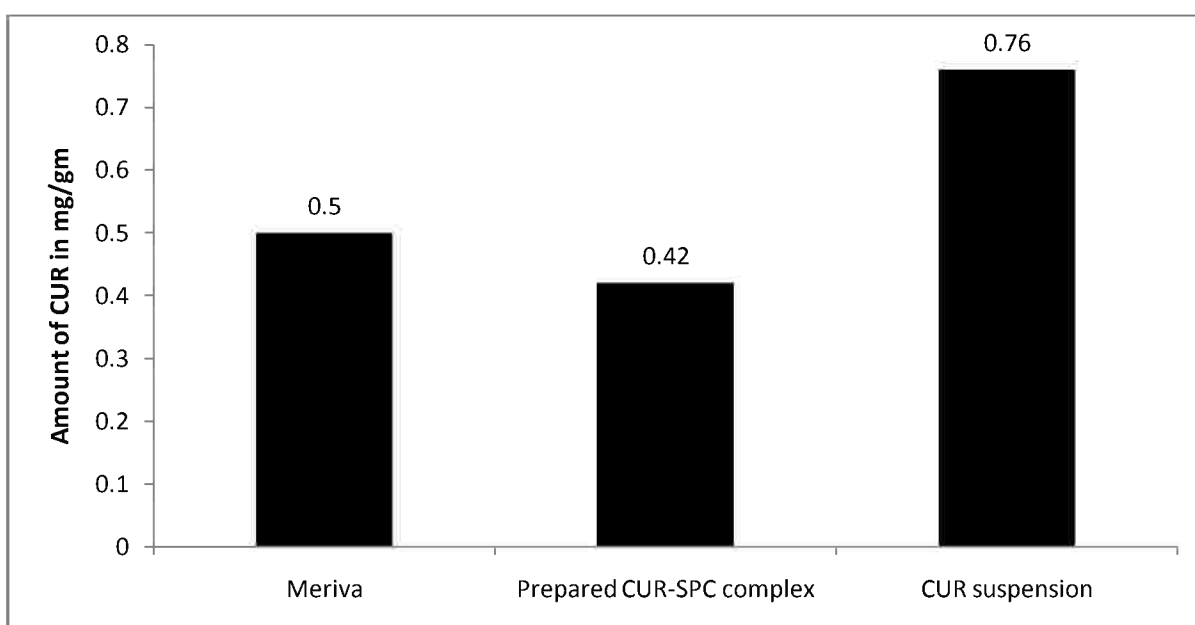


**Figure 60: Mucosal uptake for Meriva™, prepared CUR-SPC complex and CUR suspension**

#### 4.5. Preparation of fill formulations of CUR-SPC complex in softgels

Formulation development for CUR-SPC complex powder was required to enhance the dissolution profile for CUR to line with the pharmacopeial limits (i.e. Not less than 75% after 1 hours in 1% aqueous SLS).

Many advantages to select soft gelatin capsule as a dosage form for development of CUR-SPC complex powder. One of them is the ability to increase the dose of CUR in softgels to reach 200 mg CUR per capsule compared to only 100 mg CUR per hard gelatin capsule. The second advantage is using several bioactive excipients as poloxamers, polyethylene glycol, cremophore RH 40 and cremophore EL because of their reported inhibitory effect on CYP 3A4<sup>(208, 209)</sup> which affect on the intestinal metabolism for CUR<sup>(137)</sup>, hence promotes its systematic bioavailability.

From previous work in the part one, Class III<sub>a</sub> of lipid formulation classification system comprising from hydrophilic surfactant and LCT/MCT oil was selected to

formulate CUR-SPC complex powder as a soft gelatin capsule. From this point of view, CUR-SPC complex softgel was formulated in two different techniques:

1. Dispersion of CUR-SPC complex powder in oily vehicle.
2. Application of CUR-SPC complex in the semi-solid form in a hydrophilic vehicle.

#### **4.5.1. Preparation of CUR-SPC complex powder in softgels.**

Upon preparation of CUR-SPC complex powder in softgel, only 500 mg of complex powder serving 100 mg CUR in addition to 1 gm oily vehicle were utilized in the formulation development of CUR-SPC complex softgel.

Different hydrophilic surfactants with different concentrations including CRM EL, CRM RH 40 and KLS P 124 and different oily vehicles were used to optimize fill formulation of CUR-SPC complex powder to enhance the dissolution profile of CUR to line with pharmacopeial specifications. It must be mentioned that presence of antioxidant material as BHT in the dispersion medium is to prevent any oxidation process that could be taken place for hydrophilic surfactant as reported in the part one.

It was shown experimentally in F1 that optimum ratio between CUR-SPC complex powder and oil to be encapsulated in softgel was (1:2). CRM EL was used in F2, F3, and F4 in 10%, 20% and 40% respectively in the presence of Miglyol 812<sup>TM</sup> as oily vehicle to show the effect of applying different concentration of CRM EL on the dissolution of CUR. It was observed experimentally that there is an increase in the viscosity of the fill with the increase in the concentration of CRM EL to reach 4780 cP, Thus there was a disability to encapsulate fill formulation containing 40% CRM EL in a softgel. On other hand, In F5 20% CRM EL was used in the presence of soya bean oil instead of Miglyol 812<sup>TM</sup> to show the effect of change the type of oily vehicle on the dissolution rate of CUR-SPC complex powder.

In F6 and F7, 20% CRM RH 40 which has higher HLB value was utilized instead of CRM EL to show the effect of application of another surfactant from the same chemical group on the dissolution of CUR from its complexed structure with different oily vehicle Miglyol 812<sup>TM</sup> and soya bean oil respectively.

In F8 and F9, KLS P 124 was used in concentration 20% and 40% respectively with Miglyol 812<sup>TM</sup> to study the effect of applying different concentration of liquid poloxamar on dissolution profile of curcumin from CUR-SPC complex.

#### **4.5.2. Preparation of CUR-SPC semi solid complex in softgel.**

Utilizing the semi solid form of CUR-SPC is encountered to be a new method in the preparation of CUR-SPC complex softgels. This method provides several advantages which are illustrated in Table 15 over the conventional method for preparation of CUR-SPC complex in the powder form.

**Table 15: Comparison between advantages of preparing CUR-SPC semi solid complex over CUR-SPC complex powder in softgels**

<b>Point of comparison</b>	<b>CUR-SPC semi solid complex form</b>	<b>CUR-SPC complex powder form</b>
<b>Vehicles/fillers</b>	Applicability to use liquid vehicle instead of fillers to fluidize the semi solid form of the prepared complex.	Using of 40% of filler to prepare a powder form of the complex which in turns decrease CUR content.
<b>Dosing of CUR</b>	Ability to increase the CUR content in the softgel to reach 200 mg.	Only 100 mg CUR could be used in softgel as a dosage form for CUR-SPC complex powder.
<b>Application on large production scale</b>	Few steps and equipments with low possibilities for material loss are required to prepare the fill content for softgel.	More processes and equipments with high possibilities for material loss are required to prepare fill content for softgel.

To preserve CUR-SPC complex structure in a fluid form, the used liquefied vehicle must not affect the complex integrity and this could be achieved by using either lipophilic or hydrophilic vehicle with hydrophilic surfactant.

Due to limited available data on the solubility of SPC in different hydrophilic/lipophilic vehicles and surfactants, selection criteria for vehicle was depend on the available solubility data of CUR in different vehicles and surfactants as shown Table 13. From the solubility data, components of CUR-SPC semi solid complex was illustrated in Table 12. In addition, BHT was added as antioxidant material to avoid any autoxidation process for CRM EL or KLS P 124.

## **4.6. Characterization of fill formulations for CUR-SPC complex**

### **4.6.1. Evaluation of *in vitro* dissolution test.**

In-vitro dissolution results for the fill formulations of CUR-SPC complex powder (F1 – F9) and CUR-SPC semisolid complex (F10 - F13) were graphically illustrated in (Figure 61). F1 showed a relative low dissolution result that reaches 13% which may be attributed to the high affinity of CUR-SPC complex powder towards lipophilic vehicle (pure Miglyol oil).

Dissolution results of CUR-SPC complex powder was shown to be enhanced on increasing the concentration of hydrophilic surfactant (i.e. CRM EL) where 10%, 20% and 40% were used at F2, F3 and F4 respectively. Although dissolution results of F4 were better than results of F2 and F3, it was excluded from further studies due to observed high viscosity of the prepared formula.

On the other hand, different hydrophilic surfactants like CRM RH 40 and KLS P 124 were utilized to show the effect of change the type of surfactant on the dissolution of CUR-SPC complex having the same concentration as shown in F3, F6 and F 8 where 20% CRM EL, 20% CRM RH 40 and 20% KLS P 124 were used to the latter formulations respectively.

It was observed that there were no difference between 20% CRM EL and 20% CRM RH 40. Also, using 20% KLS P 124 showed better results than other types of surfactants, from this result 40% of KLS P 124 were examined in F9 which gave the highest dissolution for CUR-SPC reaching to 87% after 60 mins which could be accepted according to the USP tolerance.

For selecting oily vehicle, LCT (i.e. soya bean oil) and MCT (i.e. Miglyol 812<sup>TM</sup>) were examined between different formulations with the same type of surfactant and the same concentrations as shown on using 20% CRM EL at F3, F5 and 20% CRM RH 40 at F6,F7. Results were shown that using Miglyol 812<sup>TM</sup> was greatly enhanced the dissolution of CUR-SPC complex than using soya bean oil; this may be due to relative solubility of CUR in Miglyol 812<sup>TM</sup> rather than soya bean oil as shown in Table 13.

For CUR-SPC semisolid complex, lipophilic and hydrophilic vehicles were examined as a carrier for the prepared complex. For lipophilic vehicles; Results showed that using MCT (i.e. Miglyol 812) at F10 gave better dissolution behavior over F11 and F 12 containing oleic acid and castor oil respectively. This may be due to the relative high CUR solubility in Miglyol 812<sup>TM</sup> over castor oil. On other hand, hydrophilic vehicle was used compromising from PEG 400 and CRM EL giving the highest dissolution results over other lipophilic formulations.

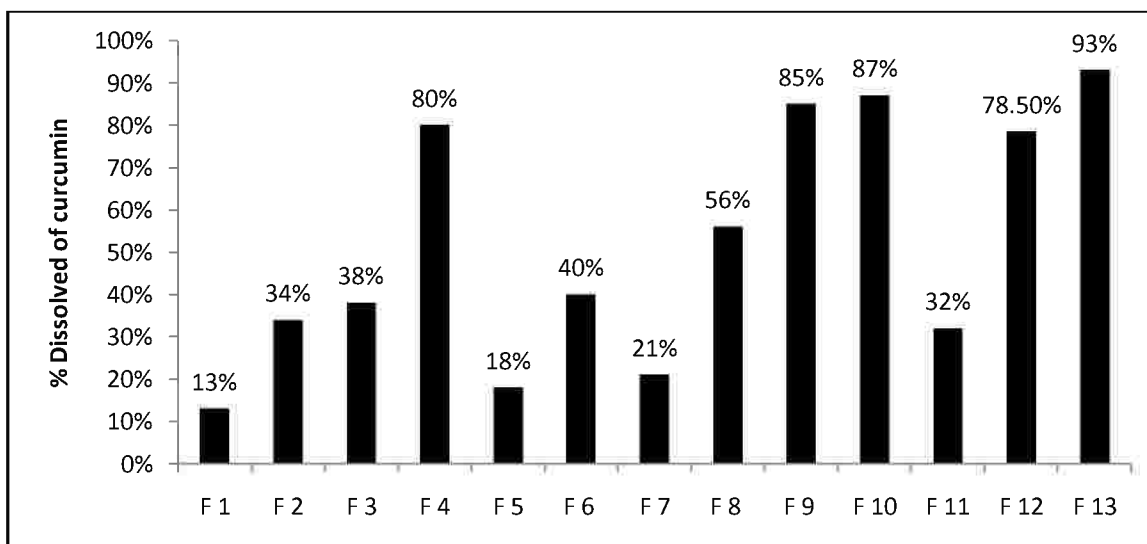


**Figure 61: *In vitro* dissolution results of CUR fill formulations after 60 mins in aqueous 1% SLS.**

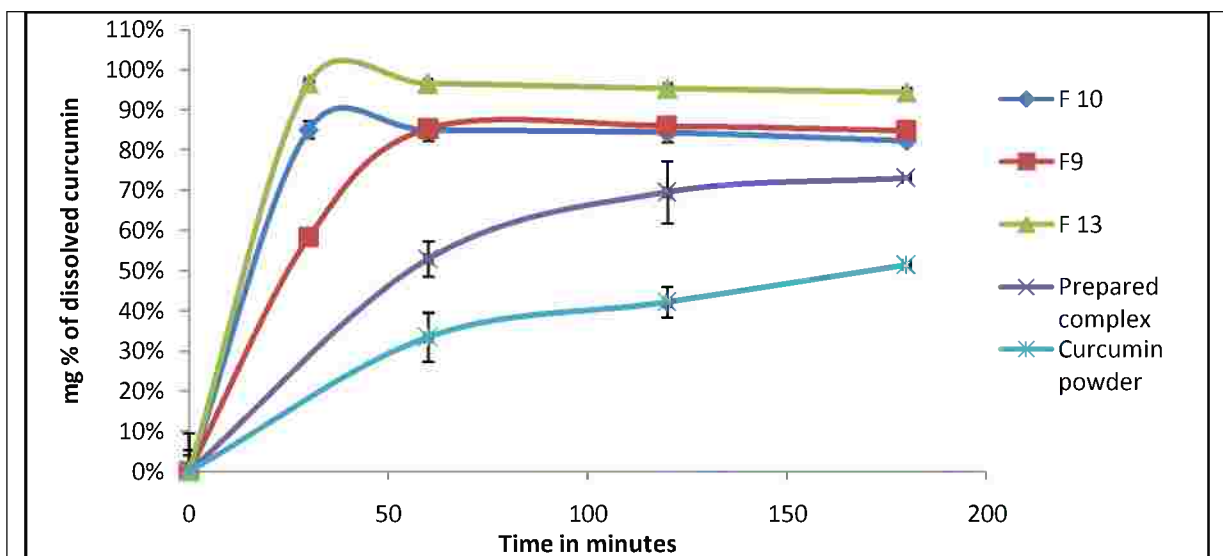


**Figure 62: Comparative dissolution pattern among pure CUR, Prepared complex, F9, F10 and F13 in aqueous 1% SLS.**

From the above mentioned results F9, F10 and F13 were selected for further dissolution pattern study and shelf stability study in softgels. In (Figure 62), it was shown the dissolution enhancement for CUR was achieved by preparation of its complex with SPC, and the dissolution of the latter was greatly improved by further formulations in F9, F10 and F13. Also it was observed an immediate dissolution for CUR in F10, F13 after 30 mins if compared with F9. This may be due to the liquefied form of the complex which promotes better the dissolution behavior than the powder one.

#### 4.6.2. Transmission electron microscope (TEM)

As shown in (Figure 63), F 10 dispersion in the water leads to the formation of phytosomal form of CUR resembling to those obtained in (Figure 13). However, in (Figure 64), it was shown a presence of vesicles composed of CUR-SPC phytosomal structure dissolved in PEG 400.



**Figure 63: Transmission electron microscopic photograph of F10 with 20 folds dilutions in distilled water before shelf stability.**

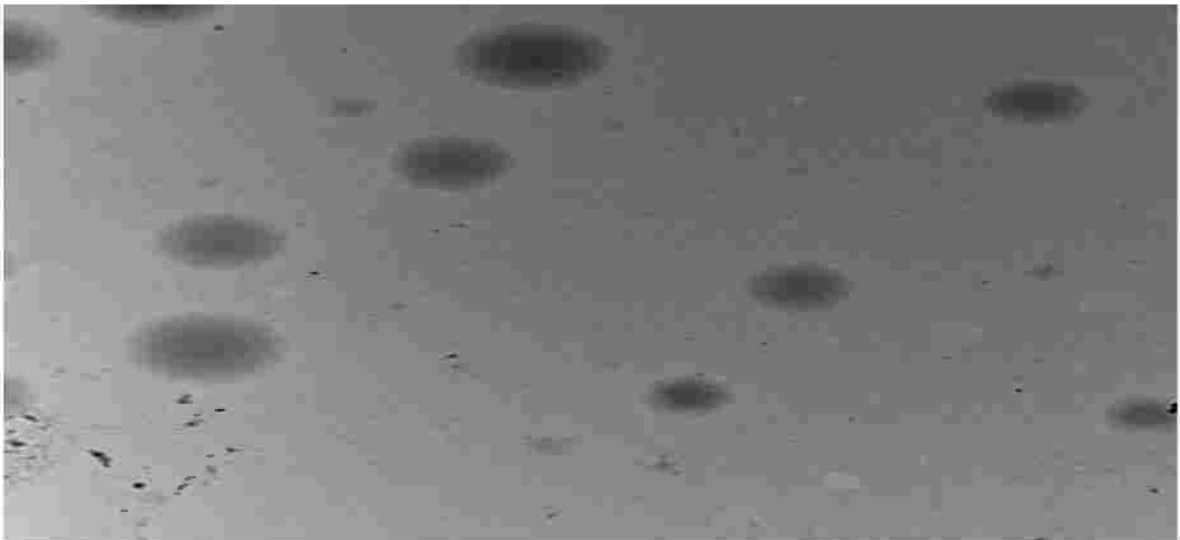


**Figure 64: Transmission electron microscopic photograph of F13 with 20 folds dilutions in distilled water before shelf stability.**

## **4.7. Shelf stability for CUR-SPC fill formulations.**

### **4.7.1. *In vitro* dissolution study**

As shown in (Figures 65 and 66), dissolution rate of CUR-SPC complex was sharply decreased for F9 and F10 if compared to its results at zero time. This is may be due to the limited solubility of CUR in oily vehicles used in the preparation of such formulations and liability of SPC towards the oily vehicle leading to salting out of CUR. Salting out of CUR affects on the CUR-SPC complex integrity leading to a decrease in the dissolution profile of CUR.

On the other hand, dissolution profile for F 13 shown in (Figure 67) was not affected after storage for 3 months in a softgel. This may be explained by the compatibility of PEG 400 with CUR-SPC complex. Thus, application of PEG 400 as hydrophilic vehicle to CUR-SPC complex doesn't affect on the complex integrity between CUR and SPC. It must be noticed that the latter suggestions will be confirmed by further studies.

### **4.7.2. Transmission electron microscope (TEM)**

TEM photographs for F10 can support our suggestions about salting out idea of CUR from CUR-SPC complex. At (Figure 68), showed a transparent vesicle with thin irregular membrane which may be referred to phospholipid layer and a small black spot at the middle of each vesicle which may be referred to salted out CUR from the complex. These findings support the idea of possible destruction of CUR-SPC complex which in turns affect on the dissolution behavior of F 10.

On the other hand, TEM photographs for F13 in (Figure 69) showed opaque vesicles with regular surface. These vesicles may be referred to CUR-SPC complex solubilized on PEG 400. On comparison to TEM photos of prepared phytosome powder in (Figure 13), a difference in vesicular shape was observed which may be attributed to high solubility of CUR in PEG 400 and a continuous dynamic movement of solubilized CUR particles which give its ability to appear inside the hallow phospholipid structure. The integrity of phytosome in F13 will be confirmed by zeta potential measurements.

### **4.7.3. Zeta potential measurements**

No change in ZP measurement for aqueous dispersion of F13 ( $-38.8 \pm 3.48$  mV) compared to that for CUR-SPC complex ( $-35.4 \pm 2.45$  mV) was observed which indicates good stability. It is concluded that PEG 400 doesn't affect the integrity of CUR-SPC complex. This finding was in agreement with the finding that obtained by both dissolution results and TEM for F13 as shown in (Figure 70).

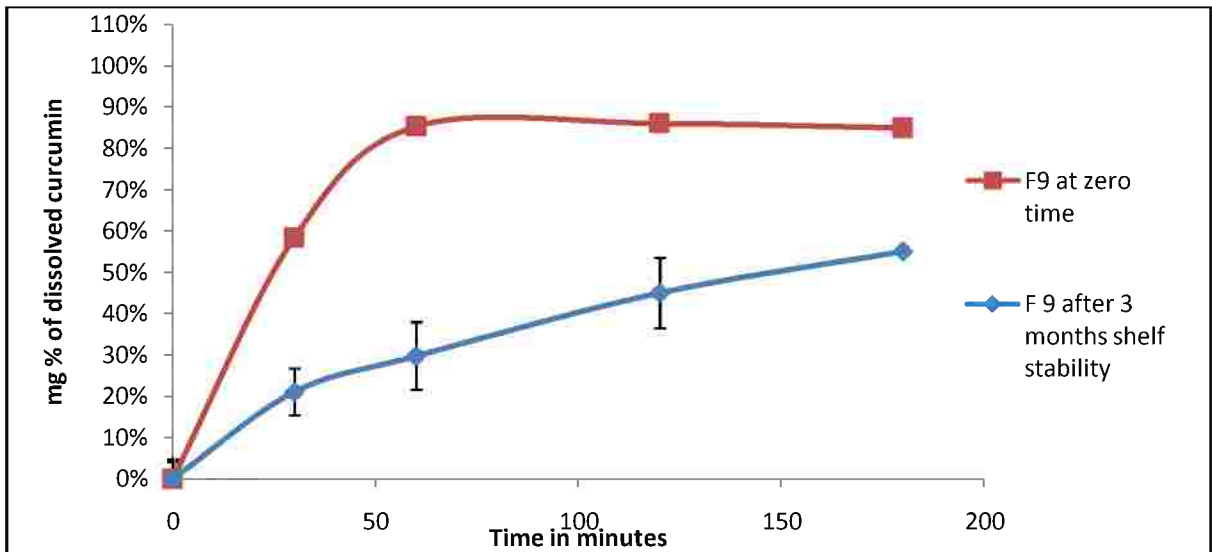


**Figure 65: Comparative dissolution profile of F9 at zero time and after 3 months shelf stability.**

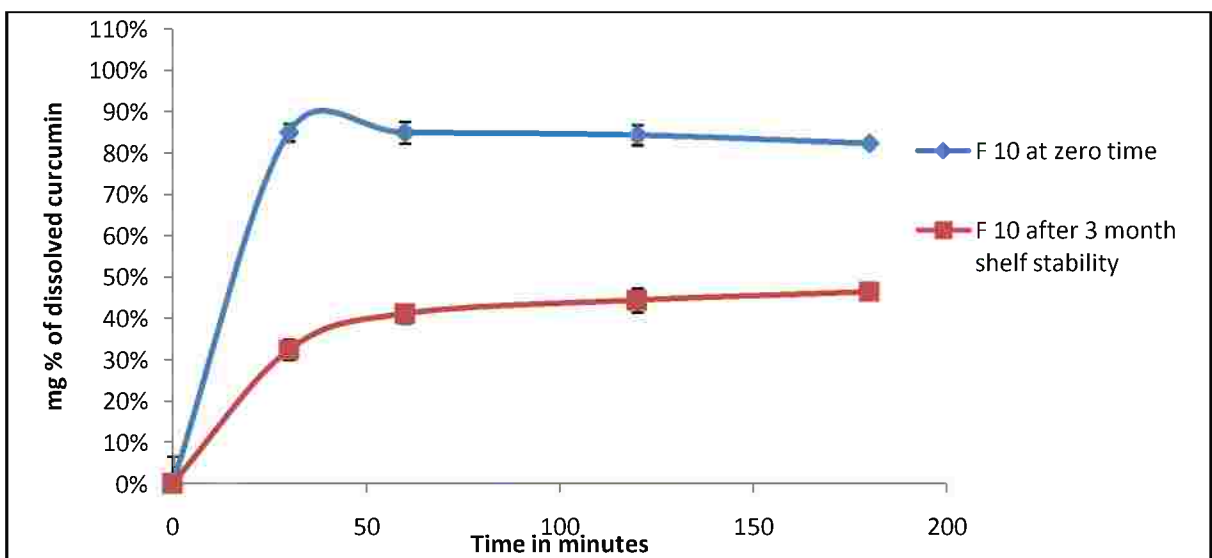


**Figure 66: Comparative dissolution profile of F10 at zero time and after 3 months shelf stability.**

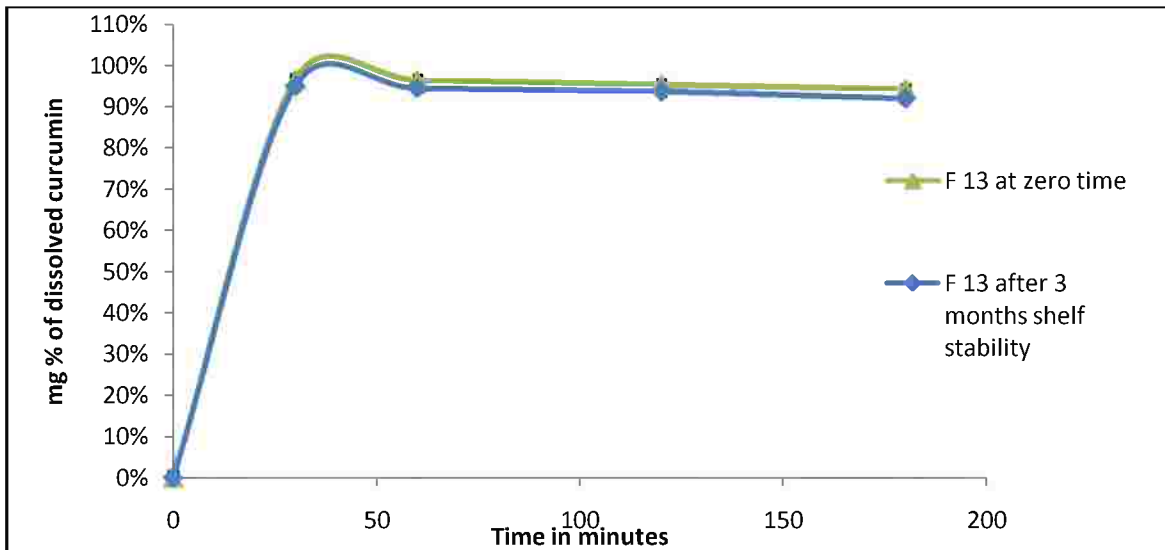


**Figure 67: Comparative dissolution profile of F13 at zero time and after 3 months shelf stability.**

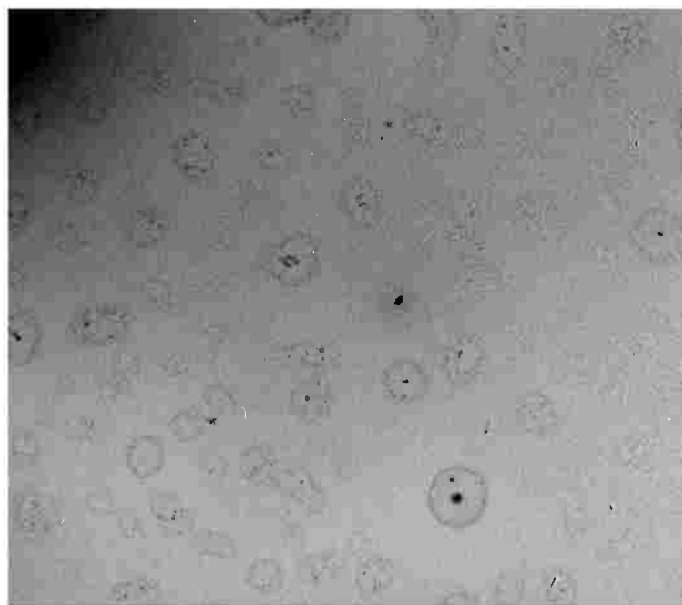


**Figure 68: Transmission electron microscopic photograph of F10 with 20 folds dilutions in distilled water after shelf stability.**

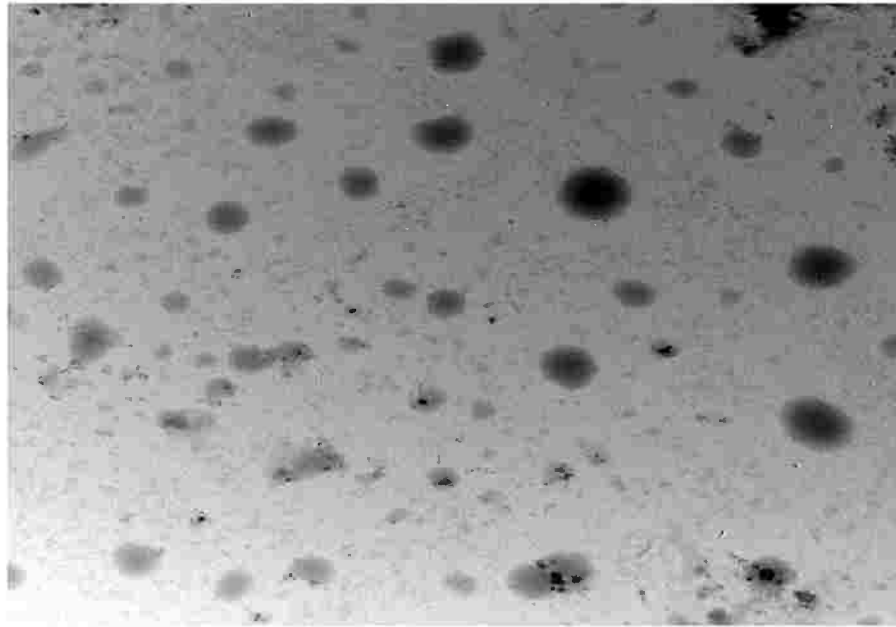


**Figure 69: Transmission electron microscopic photograph of F13 with 20 folds dilution in distilled water after shelf stability.**

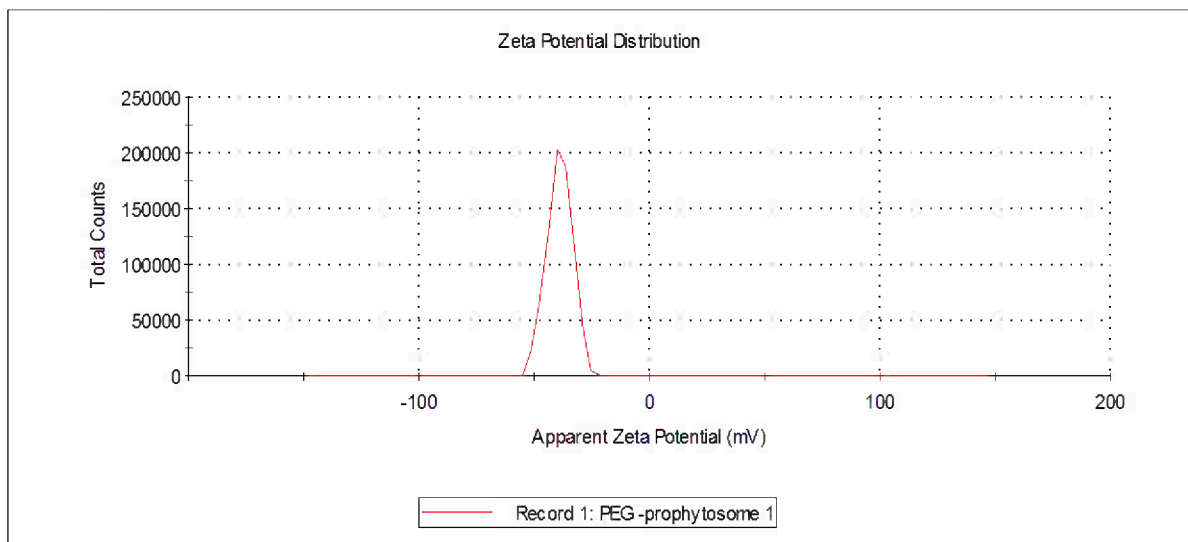


**Figure 70: Zeta potential measurement for F13 after dispersion in distilled water.**